

Charge order and possible bias-induced metastable state in the organic conductor β -(*meso*-DMBEDT-TTF)₂PF₆: effects of structural distortion

Y Tanaka and K Yonemitsu

Department of Physics, Chuo University, Bunkyo-ku, Tokyo 112-8551, Japan
JST, CREST, Chiyoda-ku, Tokyo 102-0076, Japan

E-mail: yasuhiro@phys.chuo-u.ac.jp

Abstract. We theoretically investigate charge order and nonlinear conduction in a quasi-two-dimensional organic conductor β -(*meso*-DMBEDT-TTF)₂PF₆ [DMBEDT-TTF=dimethylbis(ethylenedithio)tetrathiafulvalene]. Within the Hartree-Fock approximation, we study effects of structural distortion on the experimentally observed checkerboard charge order and its bias-induced melting by using an extended Hubbard model with Peierls- and Holstein-types of electron-lattice interactions. The structural distortion is important in realizing the charge order. The current-voltage characteristics obtained by a nonequilibrium Green's function method indicate that a charge-ordered insulating state changes into a conductive state. Although the charge order and lattice distortions are largely suppressed at a threshold voltage, they remain finite even in the conductive state. We discuss the relevance of the results to experimental observations, especially to a possible bias-induced metastable state.

PACS numbers: 71.30.+h, 72.20.Ht, 77.22.Jp, 71.10.Fd

1. Introduction

Organic conductors offer intriguing subjects of low-dimensional correlated electron systems in which various electronic states emerge at low temperatures[1, 2]. In addition to the origin of such phases in thermal equilibrium condition, nonequilibrium properties induced by external stimuli have attracted much attention recently[3, 4]. For example, photoinduced phase transitions[5, 6, 7] and nonlinear conduction phenomena[8, 9, 10, 11], which have been observed mainly in Mott insulators and charge-ordered compounds, have been intensively studied.

In the quasi-two-dimensional organic conductor β -(*meso*-DMBEDT-TTF)₂PF₆[12] [abbreviated as β -(DMeET)₂PF₆ hereafter], nonlinear conduction has been observed in a charge-ordered insulating phase[13]. The conduction layer of β -(DMeET)₂PF₆ consists of a weakly dimerized pair of neighboring donor molecules [Fig. 1(a)] and forms a 3/4-filled band. This compound shows a second-order metal-insulator transition at 90 K, where the peculiar checkerboard charge order (CCO) occurs[14, 15] [Fig. 1(b)]. This transition accompanies a structural distortion. Under pressure, the CCO is readily suppressed and superconductivity with $T_C \sim 4$ K appears[12, 16, 17].

Theoretically, Yoshimi *et al.*[18] have investigated the superconductivity by using the random phase approximation for an extended Hubbard model with on-site and nearest neighbor Coulomb interactions. They show that the CCO does not appear when they consider values of the Coulomb interactions that are determined from the intermolecular distances and the effective molecular sizes. Since their model has only electronic degrees of freedom, their result suggests that electron-lattice (e-l) interactions play an important role in stabilizing the CCO. In fact, it is experimentally known that modulation of transfer integrals and bending of molecules occur at the transition triggered by the charge disproportionation[14]. However, the effects of lattice degrees of freedom on the CCO have not been studied so far.

When the bias voltage is applied, β -(DMeET)₂PF₆ exhibits a negative differential resistance below 70 K, where the initial CCO insulating state shows a steep decrease of the resistivity[13]. Moreover, in the current-voltage characteristics, a non-monotonic behavior of the voltage drop was observed. A recent Raman spectroscopy measurement[19] indicates that the CCO melts by the bias. The time-resolved measurement shows a two-stepped sample voltage drop with a transient plateau, which suggests that there appears an electric-field-induced metastable state which is different from the normal metallic phase at high temperatures[13, 19]. Such a new phase in nonequilibrium condition is also suggested in a photoinduced state of a quasi-one-dimensional organic conductor (EDO-TTF)₂PF₆ in which strong electron-phonon interactions play an important role in its charge-ordered ground state[6, 20, 21, 22]. In a recent femtosecond electron diffraction study[22], time-dependent structural changes after the photoexcitation have been monitored and the difference between the photoinduced transient state and the low-temperature charge-ordered state has been identified. In this context, in addition to the origin of the CCO in β -(DMeET)₂PF₆, the

mechanism of the nonlinear conduction and the identification of the phases appearing by melting the CCO are intriguing subjects.

In this paper, we study the equilibrium and nonequilibrium properties of β -(DMeET)₂PF₆. We use an extended Hubbard model with two kinds of e-l couplings that are deduced from the experimental observations. The CCO becomes the ground state by these lattice distortions since the Coulomb interactions basically do not favor the checkerboard charge pattern. This state is similar to the (1100) charge order that has been discussed in quasi-one-dimensional systems by Clay *et al.*[20]. In two dimensions, a concept of the paired-electron crystal[23, 24] that consists of pairs of charge-rich sites separated by pairs of charge-poor sites, has been proposed in order to understand the ground state of interacting quarter-filled systems with e-l couplings and frustration. We investigate nonlinear conduction by applying a bias to the CCO insulating state. The bias induces a conductive state possessing a weak CCO and partial lattice distortions, which is distinct from the insulating ground state. This indicates the appearance of a metastable state different from the metallic phase at high temperatures.

This paper is organized as follows. In §2, the model Hamiltonian for β -(DMeET)₂PF₆ and the methods of calculations are presented. In §3, we show the results and their relevance to the experimental observations is discussed. §4 is devoted for summary and conclusions.

2. Model and Methods

We consider the extended Hubbard model with Peierls- and Holstein-types of e-l interactions written as

$$\begin{aligned} H = & \sum_{\langle ij \rangle \sigma} \left[(t_{i,j} + \alpha u_{i,j}) c_{i\sigma}^\dagger c_{j\sigma} + h.c. \right] \\ & + U \sum_i (n_{i\uparrow} - N_e/2)(n_{i\downarrow} - N_e/2) \\ & + \sum_{\langle ij \rangle} V_{i,j} (n_i - N_e)(n_j - N_e) + \beta \sum_i v_i (n_i - N_e) \\ & + \sum_{\langle ij \rangle} \frac{K_\alpha}{2} u_{i,j}^2 + \sum_i \frac{K_\beta}{2} v_i^2, \end{aligned} \quad (1)$$

where $\langle ij \rangle$ represents a pair of neighboring sites, $c_{i\sigma}^\dagger (c_{i\sigma})$ denotes the creation (annihilation) operator for an electron with spin σ at the i th site, $n_{i\sigma} = c_{i\sigma}^\dagger c_{i\sigma}$, $n_i = n_{i\uparrow} + n_{i\downarrow}$, and the average electron density is $N_e = 1.5$. We write the transfer integrals as $t_{i,j}$, the on-site repulsion U , and the nearest neighbor Coulomb interactions $V_{i,j}$. The coupling strength, the lattice displacement, and the elastic constant for the Peierls-type e-l interaction are denoted by α , $u_{i,j}$, and K_α , respectively, whereas those for the Hostein-type e-l interaction are written as β , v_i , and K_β . We introduce new variables by

$$y_\alpha^{i,j} = \alpha u_{i,j}, \quad (2)$$

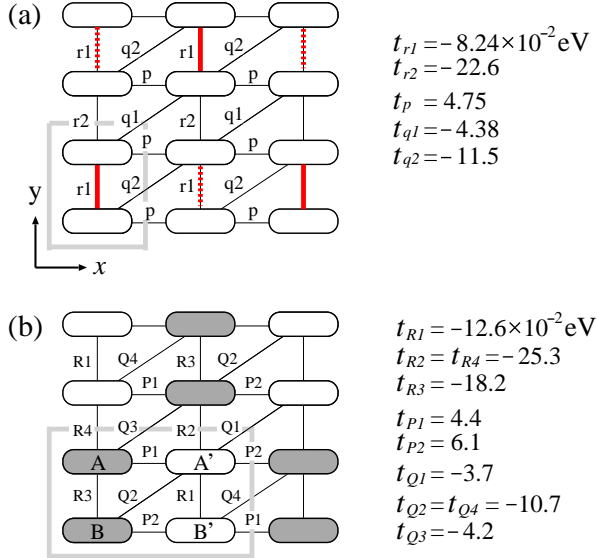


Figure 1. (Color online) Schematic representation of molecular configurations in donor layer of β -(DMeET)₂PF₆: (a) high-temperature metallic phase and (b) CCO phase. The gray rectangles indicate the unit cells. The transfer integrals estimated from the extended Hückel method[12, 15] are also shown. In (a), the red or thick solid (dashed) lines indicate the bonds on which the magnitudes of the transfer integrals are increased (decreased) by the distortions considered in the present paper. In (b), the sites A and B are hole-rich, whereas the sites A' and B' are hole-poor.

$$s_\alpha = \alpha^2 / K_\alpha, \quad (3)$$

$$y_\beta^i = \beta v_i, \quad (4)$$

$$s_\beta = \beta^2 / K_\beta. \quad (5)$$

For simplicity, we consider only one mode of displacements for each type of e-l interactions. The definition of the actual modulations of transfer integrals and on-site potentials is given below.

A schematic illustration of the high-temperature metallic phase of β -(DMeET)₂PF₆ is shown in Fig. 1(a). The unit cell contains two molecules. The charge density per molecule is uniform in this phase. The transfer integrals t_{r1} and t_{r2} are alternating on the vertical direction. The weakly dimerized molecules are connected by $r2$ bonds on which the magnitude of the transfer integrals is the largest.

In the CCO phase, there are four molecules in the unit cell as shown in Fig. 1(b). The transfer integrals are modulated by the structural distortion. The modulations on the vertical bonds are larger than those on the diagonal and horizontal bonds. In particular, $r1$ bonds in the high-temperature phase change into $R1$ and $R3$ bonds that are inequivalent ($t_{R1} > t_{R3}$). According to the X-ray diffraction measurement[14, 15], we have $d_{R2} = d_{R4} < d_{R3} \simeq d_{R1}$, where d_l denotes the distance between the neighboring molecules connected by the bond l . The intermolecular distance within a dimer is the shortest. For the diagonal and horizontal directions, the intermolecular distances are

larger than d_{R1} and d_{R3} . With these facts, we expect that $V_{r2} > V_{r1} > V_p$, V_{q1} , V_{q2} in Fig. 1(a), where V_l represents the nearest neighbor Coulomb interaction between the two sites connected by the bond l . In fact, it has been pointed out[14, 15] that, if it were not for e-l interactions, the charge order along the vertical direction should be of r-p-r-p type, where r and p represent hole-rich and -poor sites, respectively. This is because the charge pattern of the intradimer pair should be r-p, and that of the second-nearest interdimer pair should also be r-p if we consider only the Coulomb interactions that are determined by the intermolecular distances. However, the CCO is of r-r-p-p type in which the two molecules connected by $R3$ ($R1$) bonds become hole-rich (hole-poor). These considerations suggest that lattice effects are the key to understanding the CCO.

In order to take account of the structural distortion, we introduce modulations of the transfer integrals on $r1$ bonds as

$$t_{R1}^d = t_{r1} + y_\alpha, \quad (6)$$

$$t_{R3}^d = t_{r1} - y_\alpha, \quad (7)$$

where t_{R1}^d (t_{R3}^d) is the modified transfer integral located on $R1$ ($R3$) bonds in the low-temperature structure [Fig. 1(b)]. When $y_\alpha > 0$, we have $t_{R1}^d > t_{R3}^d$ that is consistent with the relation $t_{R1} > t_{R3}$ in Fig. 1(b), which is derived from the experimental result. Experimentally, the thermal contraction makes the averaged $|t|$ larger at low temperatures, thus $|t_{R1}|, |t_{R3}| > |t_{r1}|$. In essence, the modulation given by Eqs. (6) and (7) stabilizes the r-r-p-p type charge pattern in the CCO. We do not consider modulations of the other transfer integrals since they are relatively small compared to the above. In our calculations, the values of the transfer integrals $t_{i,j}$ in Eq. (1) are fixed at those in the high-temperature phase. We use $t_{r1} = -0.0824$, $t_{r2} = -0.226$, $t_p = 0.0475$, $t_{q1} = -0.0438$, and $t_{q2} = -0.115$.

For the Holstein-type e-l coupling, we assume

$$y_\beta^i = \begin{cases} y_\beta & \text{for } i \in A, B \\ -y_\beta & \text{for } i \in A', B'. \end{cases} \quad (8)$$

Experimentally, it has been known that in the CCO phase the hole-poor molecules are slightly bent, whereas the hole-rich molecules are almost flat[14]. This indicates that the modulation of the on-site potential is accompanied by the CCO.

We apply the Hartree-Fock approximation to the electron-electron interactions in Eq. (1). In the equilibrium case, we calculate the ground-state energies for several kinds of possible charge-order patterns with 2×4 or 4×2 unit cell and the periodic boundary condition for much larger systems. The stability of the CCO due to the e-l couplings is examined. The lattice distortions y_α and y_β are self-consistently determined by the Hellmann-Feynman theorem. In the nonequilibrium case, we calculate physical quantities such as the current-voltage (J - V) characteristics by using the nonequilibrium Green's function method[25, 26] which treats nonequilibrium steady states and contains the definitions of J and V . This method has been used to study the suppression of rectification[25] and the dielectric breakdown[26] in one-dimensional interacting electron

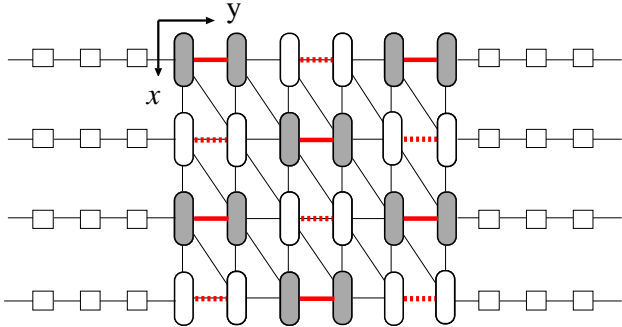


Figure 2. (Color online) Schematic model for nonequilibrium properties. The left and right electrodes are attached to the central part where the CCO is realized when the bias is absent. The y -axis (x -axis) is along (perpendicular to) the conduction direction.

systems. The results are basically consistent with those obtained by other numerical approaches which take account of the effects of quantum fluctuations[27, 28]. Although the Hartree-Fock approximation generally overestimates the stability of ordered states, the present approach is expected to capture the essential physics of nonequilibrium phenomena in β -(DMeET)₂PF₆. As shown in Fig. 2, we attach left and right semi-infinite metallic electrodes to the CCO system that is referred to as the central part. We choose the y -axis in Fig. 1(a) as the conduction direction and the qualitative results are unaltered if the bias is applied along the x -axis. We assume that the electrodes are one-dimensional and the electrons in them are noninteracting. We do not consider work-function difference at the interfaces for simplicity. For the electrodes, the wide-band limit is applied so that the retarded self-energies due to the electron transfers between the electrodes and the central part are independent of energy[29]. For finite V , we introduce the chemical potential $\mu_C = (\mu_L + \mu_R)/2$ [25] and adjust it such that the electron density of the central part is fixed at 3/4-filling. Here $\mu_L = \mu_C + V/2$ and $\mu_R = \mu_C - V/2$ are the left and right chemical potentials, respectively. Throughout the paper, we set $\gamma_L = \gamma_R = 0.1$ where γ_L (γ_R) is the coupling constant between the central part and the left (right) electrode[25, 26], and $e = \hbar = 1$. The interaction parameters U , $V_{i,j}$, s_α , and s_β are given in units of eV in the following.

3. Results

First, we discuss the ground state without the bias voltage. For the electron-electron interactions, we use $U = 0.5$, $V_{r1} = 0.23$, $V_{r2} = 0.26$, and $V_p = V_{q1} = V_{q2} = 0.2$. These parameter values are comparable to those obtained in recent *ab initio* calculations with the screening effects for typical organic compounds[30]. For $V_{i,j}$, we choose the values so that they satisfy the relation $V_{r2} > V_{r1} > V_p$, V_{q1} , V_{q2} as discussed in §2. In Fig. 3, we show the ground-state energy of the CCO for $s_\beta = 0.45$ as a function of s_α . The system size is $L_x = L_y = 32$ where L_x (L_y) is the number of sites in the x -direction (y -direction). In this figure, we also show the energies of three other phases, a paramagnetic metallic

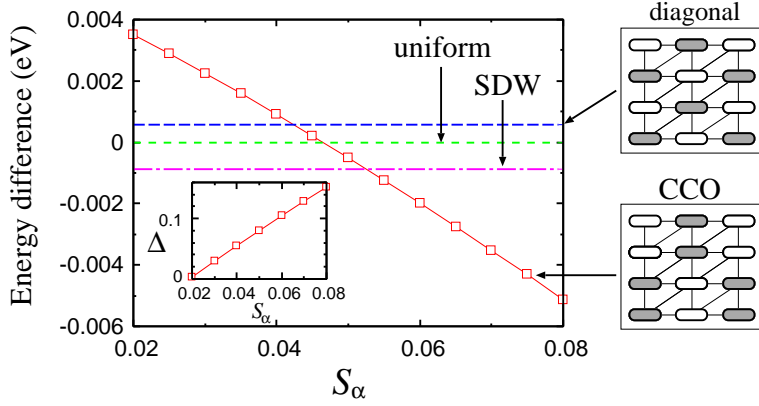


Figure 3. (Color online) Ground-state energy per site of CCO as a function of s_α for $U = 0.5$, $V_{r1} = 0.23$, $V_{r2} = 0.26$, $V_p = V_{q1} = V_{q2} = 0.2$, $s_\beta = 0.45$, and $L_x = L_y = 32$. The energies per site of the paramagnetic metallic phase (uniform), the diagonal CO, and the spin-density-wave state (SDW), which are obtained without the e-l couplings, are also shown. The energy of the uniform state is chosen to zero. The inset shows the charge gap Δ in the CCO state as a function of s_α .

state with uniform charge density, a spin-density-wave (SDW) state and a diagonal CO, which are obtained without the e-l couplings. We have confirmed that the lattice distortions in Eqs. (6)-(8) do not lower the energies of the SDW and the diagonal CO. The uniform phase is taken as a reference state and its energy is chosen to be zero. The diagonal CO has a slightly higher energy than the uniform phase. In the SDW state, the spins are antiferromagnetic along the x -axis, whereas they are ferromagnetic along the y -axis. This is consistent with the results in the random phase approximation[18], which show that the spin susceptibility has the largest peak at $\mathbf{q} = (\pi, 0)$ for $U = 0.5$. When the e-l couplings are present, the CCO becomes the ground state for $s_\alpha > 0.055$. This state has a charge gap Δ as shown in the inset of Fig. 3. In Figs. 4 and 5, we show the electron density and the lattice distortions y_α and y_β . The electron density on sites A (A') is the same as that on sites B (B'). The CCO in Fig. 3 is nonmagnetic. In fact, a CCO with an antiferromagnetic order on the hole-rich sites, which has a slightly lower energy than the nonmagnetic CCO, is also obtained as a mean-field solution. The energy difference between the two CCOs is smaller than 10^{-3} eV/site for $s_\alpha = 0.06$ and the difference decreases with increasing s_α . Because the antiferromagnetic order is an artifact of the Hartree-Fock approximation, hereafter we use the nonmagnetic CCO as the ground state when the bias voltage is applied. It should be noted that the spin configuration does not qualitatively alter the results. According to the experimental observations, the magnetic susceptibility for β -(DMeET)₂PF₆ shows gradual decrease with lowering temperatures and abruptly drops around $T = 80$ K[31]. Its temperature dependence below 80 K suggests that the system is nonmagnetic and a spin gap opens in the CCO state.

For finite bias voltage V , we set $s_\alpha = 0.075$ so that the CCO becomes the ground state for $V = 0$. The effects of the bias on the CCO are investigated by the charge

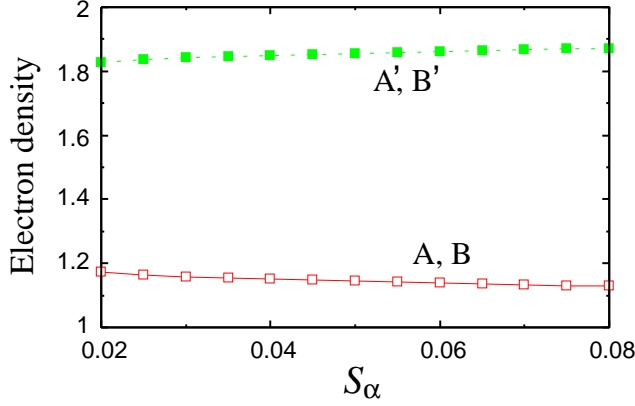


Figure 4. (Color online) Electron density of CCO phase as a function of s_α . The other parameters are the same as in Fig. 3.

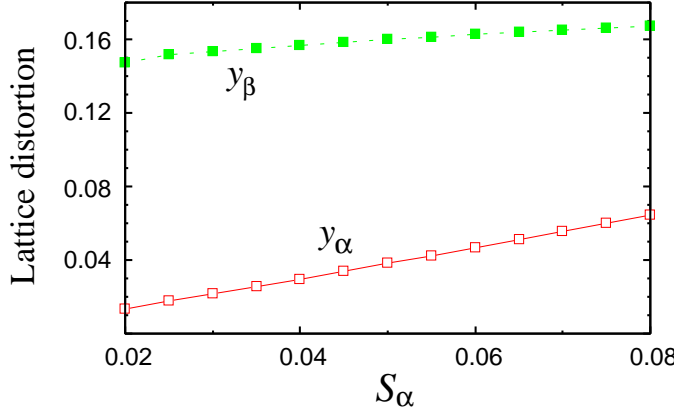


Figure 5. (Color online) Lattice distortions y_α and y_β as a function of s_α . The other parameters are the same as in Fig. 3.

structure factor $S_c(\mathbf{q})$, which is defined as

$$S_c(\mathbf{q}) = \frac{1}{N_s} \sum_{\mu, \nu} (\langle n_{\mu,1} n_{\nu,1} \rangle + \langle n_{\mu,2} n_{\nu,2} \rangle) e^{i\mathbf{q}(\mathbf{R}_\mu - \mathbf{R}_\nu)}, \quad (9)$$

where μ and ν denote indices for the unit cell shown in Fig. 1(a), 1 and 2 represent indices for the sites inside the unit cell, and \mathbf{R}_μ (\mathbf{R}_ν) is the position vector of the μ -th (ν -th) unit cell. $N_s = L_x L_y$ is the total number of sites in the central part. The wave vector that corresponds to the CCO is $\mathbf{q} = \mathbf{Q} = (\pi, \pi)$. In Fig. 6, we show the J - V characteristics and the V dependence of $S_c(\mathbf{Q})$ for $L_x = L_y = 16$. For comparison, we show the J - V curve obtained with $L_x = L_y = 12$, which gives qualitatively the same results. For small V , the current J does not flow because the charge gap opens at $V = 0$ owing to the CCO. In this region, $S_c(\mathbf{Q})$ is almost unchanged, so the CCO is robust against the bias. With increasing V , J abruptly increases at $V = V_{th} \sim 0.4$, where the CCO changes into a conductive state. Although $S_c(\mathbf{Q})$ largely decreases around $V = V_{th}$, it remains finite even in $V > V_{th}$, which means that the CCO is not completely destroyed in the conductive state. In Fig. 7, we show the lattice distortions

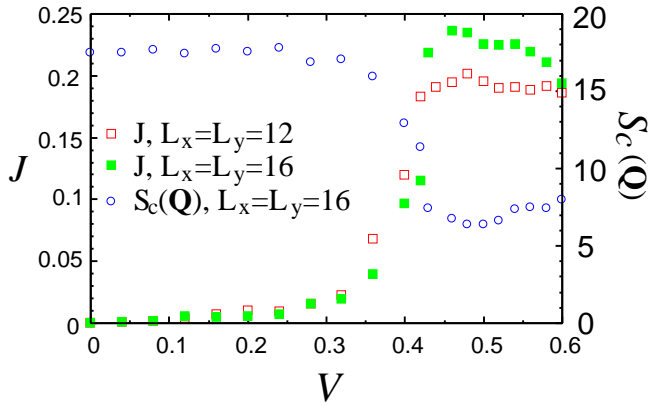


Figure 6. (Color online) J - V characteristics and V dependence of charge structure factor $S_c(\mathbf{Q})$ for $L_x = L_y = 16$ with $s_\alpha = 0.075$. J - V curve for $L_x = L_y = 12$ is also shown. The other parameters are the same as those in Fig. 3.

y_α and y_β as a function of V . Similar to the V dependence of $S_c(\mathbf{Q})$, y_α and y_β do not show noticeable change for $V < V_{th}$. At $V = V_{th}$, both distortions are suppressed. In particular, the y_α -distortion almost disappears for $V > V_{th}$, whereas the y_β -distortion survives. In equilibrium conditions, the CCO has a finite gap Δ as shown in Fig. 3. However, Δ becomes very small when y_α decreases. When the bias is applied, the initial insulating CCO switches to the conductive state by the suppression of the y_α -distortion. The weak CCO survives owing to the partial y_β -distortion, so that the bias-induced state is different from the uniform phase or the CCO at $V = 0$. In Fig. 8, we show the density of states $D(E)$ for different values of V . For $V = 0$, there is no state around $E = \mu_C$ because the charge gap opens. For $V = 0.2$, the gap structure in $D(E)$ still exists since the CCO and the lattice distortions at $V = 0$ are robust against the bias for small V . When $V = 0.5 > V_{th}$, the gap at $E = \mu_C$ disappears, which indicates that the weak CCO has the conduction property. In Fig. 6, the current J begins to decrease when V approaches half the bandwidth $W = 1.29$. This is because the number of one-particle states that have large contributions to the current J decreases for $V > W/2$ [26]. In other words, the tilting of the band by the applied bias becomes large, so that the ballistic transport is suppressed. Effects of the inelastic scattering in the central part, which are not considered in the present calculations, will modify the J - V curve in such a large V region.

Our results indicate the appearance of a bias-induced metastable state accompanied by a weak CCO. This state has only the Holstein-type distortion, which is weakened compared to the case with $V = 0$. Experimentally, the time-resolved voltage measurement[13] has shown that a two-stepped sample voltage drop with a transient plateau occurs below 70 K, which indicates that a metastable state actually exists. Such a two-stepped structure is also observed in the J - V characteristics[13]. According to the Raman spectroscopy measurement[19], in this transient metastable state the modes that are characteristic of the charge disproportionation almost disappear, so that the

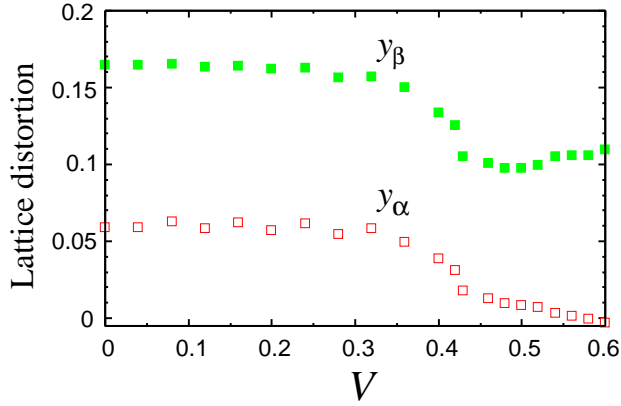


Figure 7. (Color online) Lattice distortions y_α and y_β as a function of V . The parameters are the same as those in Fig. 6.

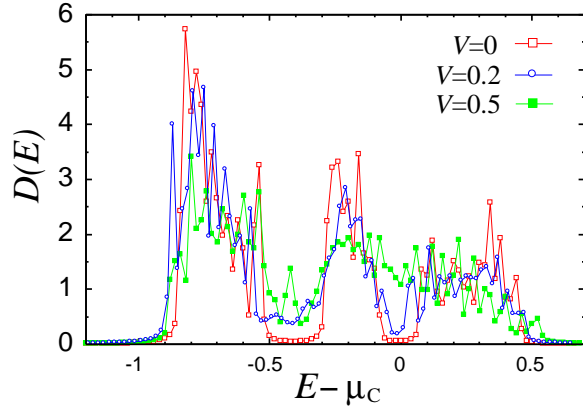


Figure 8. (Color online) Density of states for $V = 0, 0.2$, and 0.5 . The parameters are the same as those in Fig. 6.

metastable state is ascribed to the charge fluctuations. At present, it is difficult to compare our results directly to the experimental observations. Effects of the charge fluctuations that are ignored in the Hartree-Fock approximation may be important. The lattice modulation of β -(DMeET)₂PF₆ may be more complex than that considered in the present paper. In any case, our results suggest that the weak CCO has only the Holstein-type distortion in the metastable state. If we calculate the electronic state for $V = 0$ by using values of the Peierls-type and Holstein-type distortions in the metastable state, the resulting CCO has a metallic band structure. This originates from the suppression of the Peierls-type distortion. In this state, the values of $D(E)$ around $E = \mu_C$ are comparable to those at $V = 0.5$ in Fig. 8. The applied bias converts the insulating CCO into the conductive CCO. Our results may be related to the photoinduced structural changes in (EDO-TTF)₂PF₆ which exhibits the (1100) charge order at low temperatures. This charge order is triggered by displacements and bending of the EDO-TTF molecules, which corresponds to the Peierls- and Holstein-types of e-l couplings, respectively[20, 21]. The femtosecond electron diffraction study

for (EDO-TTF)₂PF₆ has shown that the photoexcitation induces the metastable state mainly through the suppression of the molecular displacements, whereas the molecular bendings do not show noticeable change[22]. More structural information such as X-ray diffraction data for the present material in the presence of the bias voltage may clarify the nature of this novel nonequilibrium phase.

4. Summary

We investigate effects of the e-l couplings on the equilibrium and nonequilibrium properties of β -(DMeET)₂PF₆. We have shown that the CCO that is peculiar to this compound is obtained by the extended Hubbard model with two kinds of e-l interactions that originate from molecular displacements and deformations. The e-l couplings are important in stabilizing the CCO. The applied bias changes the initial insulating CCO into a conductive state with the weak CCO that emerges by the disappearance of the Peierls-type distortion. This indicates the presence of a bias-induced metastable state different from the high-temperature metallic state. These results suggest that the lattice degrees of freedom play a key role in determining the conduction property in β -(DMeET)₂PF₆.

Acknowledgments

This work was supported by a Grant-in-Aid for Young Scientists (B) (Grant No. 12019365) from the Ministry of Education, Culture, Sports, Science and Technology of Japan.

References

- [1] Ishiguro T, Yamaji K, and Saito G 1998 *Organic Superconductors* (Berlin: Springer-Verlag)
- [2] Seo H, Hotta C, and Fukuyama H 2004 *Chem. Rev.* **104** 5005
- [3] Yonemitsu K and Nasu K 2008 *Phys. Rep.* **465** 1
- [4] Mori T, Terasaki I, and Mori H 2007 *J. Mater. Chem.* **17** 4343
- [5] Iwai S, Yamamoto K, Kashiwazaki A, Hiramatsu F, Nakaya H, Kawakami Y, Yakushi K, Okamoto H, Mori H, and Nishio Y 2007 *Phys. Rev. Lett.* **98** 097402
- [6] Onda K, Ogiara S, Yonemitsu K, Maeshima N, Ishikawa T, Okimoto Y, Shao X, Nakano Y, Yamochi H, Saito G, and Koshihara S 2008 *Phys. Rev. Lett.* **101** 067403
- [7] Kawakami Y, Iwai S, Fukatsu T, Miura M, Yoneyama N, Sasaki T, and Kobayashi N 2009 *Phys. Rev. Lett.* **103** 066403
- [8] Kumai R, Okimoto Y, and Tokura Y 1999 *Science* **284** 1645
- [9] Sawano F, Terasaki I, Mori H, Mori T, Watanabe M, Ikeda N, Nogami Y, and Noda Y 2005 *Nature* **437** 522
- [10] Takahide Y, Konoike T, Enomoto K, Nishimura M, Terashima T, Uji S, and Yamamoto H M 2006 *Phys. Rev. Lett.* **96** 136602
- [11] Mori T, Bando Y, Kawamoto T, Terasaki I, Takimiya K, and Otsubo T 2008 *Phys. Rev. Lett.* **100** 037001
- [12] Kimura S, Maejima T, Suzuki H, Chiba R, Mori H, Kawamoto T, Mori T, Moriyama H, Nishio Y, and Kajita K 2004 *Chem. Commun.* 2454

- [13] Niizeki S, Yoshikane F, Kohno K, Takahashi K, Mori H, Bando Y, Kawamoto T, and Mori T 2008 *J. Phys. Soc. Japan* **77** 073710
- [14] Kimura S, Suzuki H, Maejima T, Mori H, Yamaura J, Kakiuchi T, Sawa H, and Moriyama H 2006 *J. Am. Chem. Soc.* **128** 1456
- [15] Mori H 2006 *J. Phys. Soc. Japan* **75** 051003
- [16] Tanaka M, Yamamoto K, Uruichi M, Yamamoto T, Yakushi K, Kimura S, and Mori H 2008 *J. Phys. Soc. Japan* **77** 024714
- [17] Morinaka N *et al* 2009 *Phys. Rev. B* **80** 092508
- [18] Yoshimi K, Nakamura M, and Mori H 2007 *J. Phys. Soc. Japan* **76** 024706
- [19] Niizeki S, Asano T, Takahashi K, Mori H, Matsuzaki H, Okamoto H, and Nishio Y 2010 *Physica B* **405** S37
- [20] Clay R T, Mazumdar S, and Campbell D K 2003 *Phys. Rev. B* **67** 115121
- [21] Yonemitsu K and Maeshima N 2007 *Phys. Rev. B* **76** 075105
- [22] M. Gao *et al* 2013 *Nature* **496** 343
- [23] Li H, Clay R T, and Mazumdar S 2010 *J. Phys.: Condens. Matter* **22** 272201
- [24] Dayal S, Clay R T, Li H, and Mazumdar S 2011 *Phys. Rev. B* **83** 245106
- [25] Yonemitsu K 2009 *J. Phys. Soc. Japan* **78** 054705
- [26] Tanaka Y and Yonemitsu K 2011 *Phys. Rev. B* **83** 085113
- [27] Yonemitsu K, Maeshima N, and Hasegawa T 2007 *Phys. Rev. B* **76** 235118
- [28] Heidrich-Meisner F, González I, Al-Hassanieh K A, Feiguin A E, Rozenberg M J, and Dagotto E 2010 *Phys. Rev. B* **82** 205110
- [29] Jauho A P, Wingreen N S, and Meir Y 1994 *Phys. Rev. B* **50** 5528
- [30] Nakamura K, Yoshimoto Y, and Imada M 2012 *Phys. Rev. B* **86** 205117
- [31] Shikama T *et al* 2012 *Crystals* **2** 1502